Valuable Characteristic of Patlak Parametric Imaging Based on Total-Body Dynamic PET Imaging: Higher Contrast For Tumor Lesions With Respect To Hypermetabolic Tissues

Zixiang Chen
Shenzhen Institutes of Advanced Technology Chinese Academy of Sciences https://orcid.org/0000-0002-9042-4477

Yanhua Duan
Shandong Qianfoshan Hospital

Chenwei Li
Shanghai United Imaging Healthcare

Ying Wang
Shanghai United Imaging Healthcare

Yongfeng Yang
Shenzhen Institutes of Advanced Technology Chinese Academy of Sciences

Xin Liu
Shenzhen Institutes of Advanced Technology Chinese Academy of Sciences

Dong Liang
Shenzhen Institutes of Advanced Technology Chinese Academy of Sciences

Hairong Zheng
Shenzhen Institutes of Advanced Technology Chinese Academy of Sciences

Zhaoping Cheng (czpabc@163.com)
Shandong Qianfoshan Hospital

Zhanli Hu
Shenzhen Institutes of Advanced Technology Chinese Academy of Sciences

Research Article

Keywords: Total-body dynamic PET, Parametric imaging, Tumor lesion contrast

Posted Date: July 23rd, 2021

DOI: https://doi.org/10.21203/rs.3.rs-669813/v1

Valuable Characteristic of Patlak Parametric Imaging Based on Total-body Dynamic PET Imaging: Higher Contrast for Tumor Lesions with Respect to Hypermetabolic Tissues

Zixiang Chen[1,2#], Yanhua Duan[3#], Chenwei Li[4], Ying Wang[4], Yongfeng Yang[1,2], Xin Liu[1,2], Dong Liang[1,2], Hairong Zheng[1,2], Zhaoping Cheng[3*], Zhanli Hu[1,2*]

[1]Lauterbur Research Center for Biomedical Imaging, Shenzhen Institute of advanced technology, Chinese academy of science, Shenzhen 518055, China.
[2]Chinese Academy of Sciences Key Laboratory of Health Informatics, Shenzhen 518055, China.
[3]Department of PET/CT, The First Affiliated Hospital of Shandong First Medical University, Shan dong Provincial Qianfoshan Hospital, Jinan 250014, China.
[4]Central Research Institute, Shanghai United Imaging Healthcare, Shanghai 201807, China.
[#]These authors contributed equally.
[*]Author to whom any correspondence should be addressed. (Email: zl.hu@siat.ac.cn, czpabc@163.com)

Abstract

Purpose: To demonstrate the characteristics of high-contrast tumor lesions on total-body dynamic positron emission tomography (dPET) parametric images qualitatively and quantitatively.
Method: We reported the results of Patlak parametric images based on total-body dPET images of four patients with different types of tumor lesions. The contrast-to-noise ratios (CNRs) of the target tumor lesions were calculated with respect to hypermetabolic tissues, including the liver and ventricles, both on static PET and parametric images.
Results: Visual comparisons between the last frame of total-body dPET images and the generated parametric images illustrated the higher contrast of tumor lesions relative to other tissues in the patients. Visualization of the tumor lesions was reserved, while that of the livers and ventricles was diminished. The parametric images resulted in higher CNR values for the tumor lesions with respect to livers and ventricles compared to those given by dynamic PET images. The results were consistent in all the cases analyzed in this study.
Conclusion: Patlak parametric imaging provides the valuable characteristic of higher contrast for tumor lesions than hypermetabolic tissues, which helps in the clinical detection and diagnosis of tumor tissues.
Keywords: Total-body dynamic PET · Parametric imaging · Tumor lesion contrast

Introduction

Dynamic positron emission tomography (dPET) using ^{18}F-FDG has been reported as a useful medical imaging tool for the clinical diagnosis, staging and therapy monitoring of various cancers[1, 2]. However, many studies have revealed the limitations of clinical analysis based on PET images that provide the concentration radiotracer activity or standardized uptake values (SUVs), e.g., high ^{18}F-FDG accumulation can also be detected in hypermetabolic healthy tissues, which may lead to false-positive diagnostic conclusions or unprecise tumor lesion localizations[3-7]. Parametric imaging based on dPET data (dynamic scanning data of reconstructed dynamic images) is expected

to be an important graphical analysis technique for the extended application of dPET that takes the advantages of dPET over static PET[8-13]. The ability of parametric images to reveal enhanced tumor regions has been reported based on multibed whole-body dPET images[11]. In this study, we report the results of parametric imaging based on total-body dPET images of four oncological patients to investigate the clinical relevance of Patlak parametric imaging, which offers higher contrast for lesions with respect to hypermetabolic tissues such as the liver and ventricles, for more precise tumor lesion detection and oncological diagnosis.

Method and materials

Image acquisition

All dPET images in the current study were acquired using a total-body PET/computed tomography (CT) scanner (uEXPLORER, United Imaging Healthcare, China) with an acquisition time of 1 hour immediately after an intravenous injection of ^{18}F-FDG at doses of 2.95, 2.87, 2.02 and 3.02 MBq/kg. The corrected dynamic projection data were divided into 30 frames (5 s × 6, 10 s × 3, 30 s × 42, 60 s × 5, 180 s × 4 and 300 s × 8), and the dynamic images were reconstructed via 3D time-of-flight (TOF) list-mode ordered-subsets expectation maximization (OS-EM) with 3 iterations and 20 subsets. The images were reconstructed into 192 × 192 × 673 matrices with a field of view (FOV) of 600 mm and a slice thickness of 2.886 mm.

Clinical diagnostic information

The imaging analysis was based on the total-body dPET images of 4 patients with different types of tumor lesions: patient #1: a huge lesion with a maximum SUV of 17.4 was observed in the superior lobe of the right lung, and the diagnostic conclusion was a sarcomatoid carcinoma of the right lung accompanied by lymph node metastasis; patient #2: soft tissue lesion with a maximum SUV of 3.1 was seen in the superior lobe of the left lung, indicating lung adenocarcinoma; patient #3: soft tissue lesion with a maximum SUV of 16.8 was seen in the superior lobe of the right lung, indicating invasive lung adenocarcinoma, and no metabolically abnormal lymph nodes were detected; and patient #4, the middle and lower esophagus showed remarkably increased metabolism and simultaneously, swollen lymph nodes were seen in the mediastinum, which was diagnosed as esophageal adenocarcinoma accompanied by lymph node metastasis. The diagnoses of all of the above patients were pathologically confirmed by biopsy or surgery.

Blood input function

The blood input function $C_p(t)$ was extracted from a 4 × 4 × 4 volume of interest (VOI) in the thoracic aorta of every dPET image series. The extracted input functions were processed to guarantee that no remarkable noise existed in the curves.

Parametric analysis

The parametric images were calculated using the Patlak linear graphical model[14] based on the effective time frames, which was defined as the frames corresponding to the monotonously descending section of the processed blood input function. The applied Patlak model is shown in Eq. 1:

$$\frac{C(t)}{C_p(t)} = \frac{\int_{t_e}^{t} C_P(\tau)d\tau}{C_P(t)} \cdot k + b \quad (1)$$

where $C(t)$ is the measured time-activity curve (TAC) of a voxel, and t_e is the reference time point corresponding to the first effective frame. The goal of parametric imaging in this study was to

calculate the slope of the voxel-level Patlak plot (1), k, which represents the metabolic flux of the tracer, based on the measured TAC, $C(t)$, of every voxel and the blood input function, $C_p(t)$. The characteristic of high contrast for the tumor lesions with respect to hypermetabolic tissues on the parametric image is illustrated by a quantitative index, CNR[15], which is calculated by

$$CNR = \frac{\overline{VOI}_{tumor} - \overline{VOI}_{normal}}{\sqrt{\sigma_{tumor}{}^2 + \sigma_{normal}{}^2}}, \quad (2)$$

where $\overline{VOI}_{tumor}$ and $\overline{VOI}_{normal}$ are the mean image intensities of manually selected VOIs of the tumor lesions and the compared normal hypermetabolic tissues, including the liver and ventricles, respectively. σ denotes the standard deviation of the corresponding VOIs.

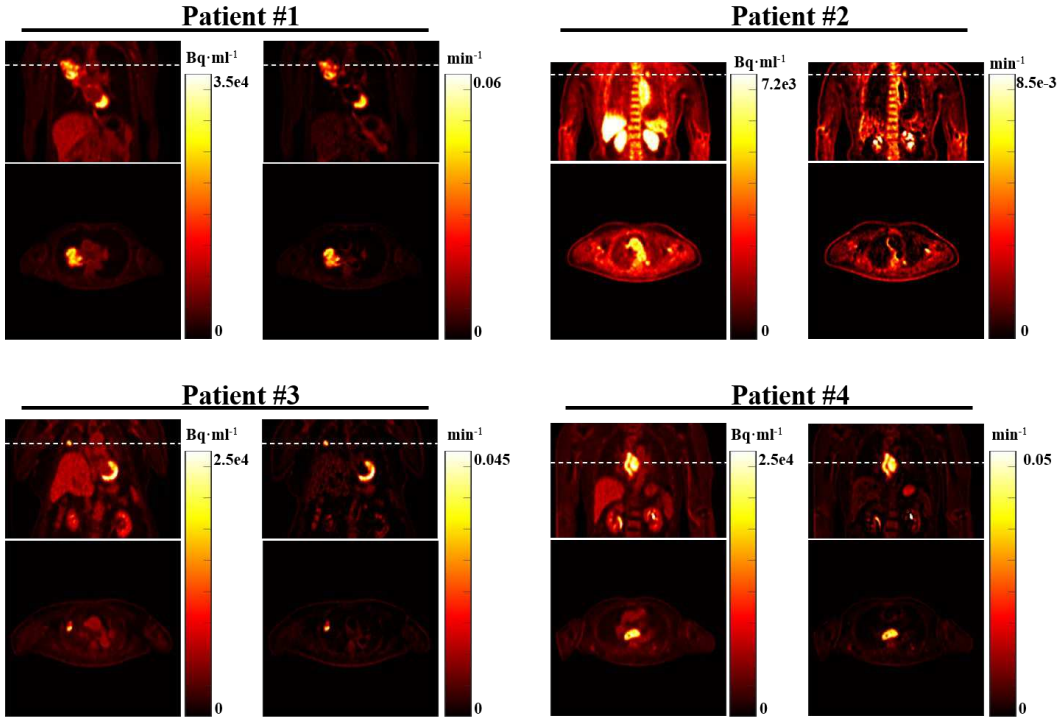

Fig. 1 Visual comparisons between the last frame of dPET images and the generated parametric image. For all four cases shown, the PET image is given on the left, and the Patlak parametric image is on the right. The transverse images represent the slices indicated by the white dashed lines in the corresponding coronary images.

Results and discussion

A visual comparison between the PET images and Patlak parametric images for the four studied patients is given in Figure 1, in which the last frame of the dynamic PET images, corresponding to a frame duration of 300 s acquired 50-55 minutes after the injection of ^{18}F-FDG, is on the left, and the parametric image calculated based on the Patlak model is on the right. Remarkable differences between these two images are observed for the hypermetabolic tissues, including the liver and heart, whose signals are strong in the PET images but significantly suppressed in the parametric images, resulting in improved visualization and enhanced contrast of the tumor lesions. This is more clearly observed for the lesion with a relatively low glucose metabolism level (Patient #2 with lung adenocarcinoma): the lesion was not obvious on the PET image compared to the liver and the adjacent aorta, while it can be clearly identified in the parametric image. The quantitative result shown in Figure 2 of the CNR of the lesion to the liver and the ventricle further demonstrates this characteristic of parametric PET images. Higher CNR values were observed with the parametric

images for all of the tumor lesions in this study, especially for patient #2.

Conclusion

In this study, we reported the results of Patlak parametric images based on total-body dPET images of four oncological patients. The visual comparisons between the PET images and the parametric images, as well as the calculated CNR results, demonstrated that the parametric images can offer improved contrast for the lesions with respect to hypermetabolic tissues. such as the liver and ventricles; this can be characteristic of parametric images can be valuable in terms of oncological diagnosis and lesion visualization.

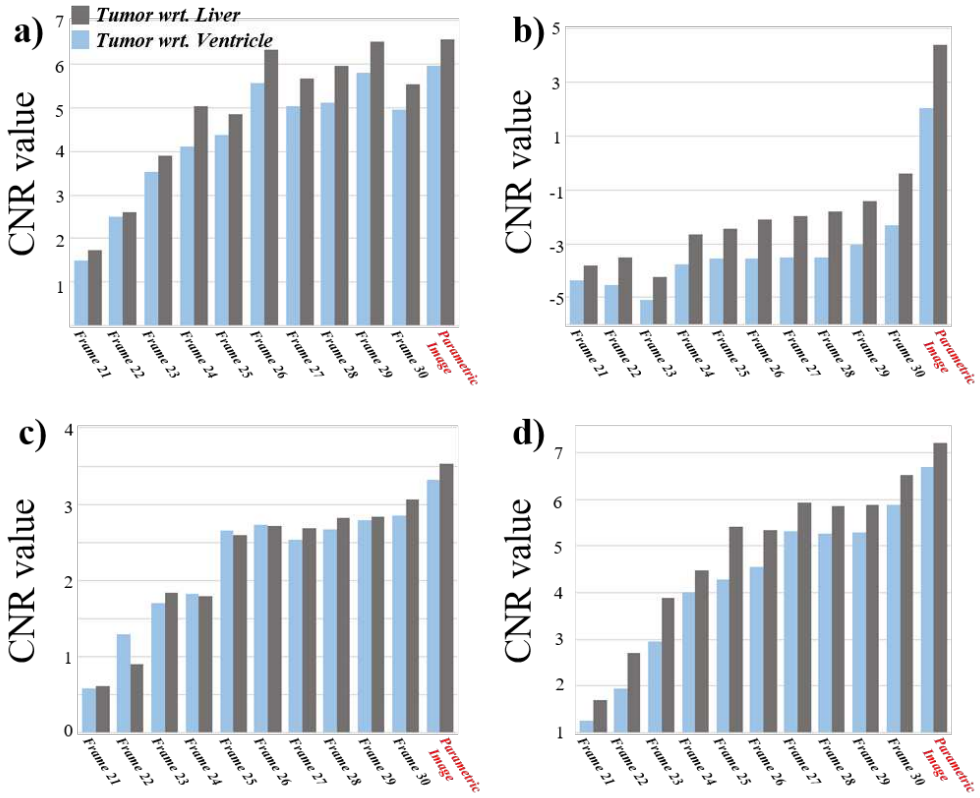

Fig. 2 The calculated CNR values of tumor lesions with respect to the liver and ventricles based on dPET images and parametric images in the four cases. a)~d) correspond to patients 1~4, respectively. Note that the negative CNR values that appear in b) are because the concentration of radiotracer activity in the tumor lesion is lower the signal of the liver or ventricles.

Declaration

Ethics approval and consent to participate

All procedures included in this study involving human participants are approved by the medical ethics committee of the First Affiliated Hospital of Shandong First Medical University. Informed consent was obtained from all individual participants included in the study.

Consent for publication

Written informed consent obtained for each subject included publication of their data and images

Availability of data and material

Patient data used in this work is provided by Department of PET/CT, The First Affiliated Hospital of Shandong First Medical University, Shandong Provincial Qianfoshan Hospital with necessary ethics approval exclusively for this study from the affiliated medical ethics committee.

Competing interests

No personal conflicts of interest relevant to this manuscript were reported.

Funding

This work was supported by the National Natural Science Foundation of China (32022042, 8 1871441), the Shenzhen Excellent Technological Innovation Talent Training Project of China (RC JC20200714114436080), the Natural Science Foundation of Guangdong Province in China (2020 A1515010733), the Guangdong Special Support Program of China (2017TQ04R395), Chinese Ac ademy of Sciences Key Laboratory of Health Informatics in China (2011DP173015).

Authors' contribution

Z Chen implemented the image analysis experiments and written most parts of the article. Y Duan was responsible for the image collection and diagnostic information providing. C Li and Y Wang were responsible for the section relevant to the introduction of the employed imaging system and the imaging method. All authors provided critical review and approved the final manuscript.

Acknowledgements

We would like to thank United Imaging Healthcare Inc. for the imaging technical support, the medical group from Shandong Provincial Qianfoshan Hospital for data supplement, and MathWorks Inc. for the software support with MATLAB R2019b.

References

[1] M. Muzi, F. O'Sullivan, D. A. Mankoff, R. K. Doot, L. A. Pierce, B. F. Kurland, H. M. Linden, and P. E. Kinahan, "Quantitative assessment of dynamic PET imaging data in cancer imaging," *Magnetic resonance imaging,* vol. 30, no. 9, pp. 1203-1215, 2012.

[2] A. Rahmim, M. A. Lodge, N. A. Karakatsanis, V. Y. Panin, Y. Zhou, A. McMillan, S. Cho, H. Zaidi, M. E. Casey, and R. L. Wahl, "Dynamic whole-body PET imaging: principles, potentials and applications," *European journal of nuclear medicine molecular imaging,* vol. 46, no. 2, pp. 501-518, 2019.

[3] J. W. Fletcher, B. Djulbegovic, H. P. Soares, B. A. Siegel, V. J. Lowe, G. H. Lyman, R. E. Coleman, R. Wahl, J. C. Paschold, and N. Avril, "Recommendations on the use of 18F-FDG PET in oncology," *Journal of Nuclear Medicine,* vol. 49, no. 3, pp. 480-508, 2008.

[4] N. M. Long, and C. S. Smith, "Causes and imaging features of false positives and false negatives on 18 F-PET/CT in oncologic imaging," *Insights into imaging,* vol. 2, no. 6, pp. 679-698, 2011.

[5] S. J. Rosenbaum, T. Lind, G. Antoch, and A. Bockisch, "False-positive FDG PET uptake− the role of PET/CT," *European radiology,* vol. 16, no. 5, pp. 1054-1065, 2006.

[6] P. D. Shreve, Y. Anzai, and R. L. Wahl, "Pitfalls in oncologic diagnosis with FDG PET imaging: physiologic and benign variants," *Radiographics,* vol. 19, no. 1, pp. 61-77, 1999.

[7] G. Williams, and G. M. Kolodny, "Method for decreasing uptake of 18F-FDG by hypermetabolic brown adipose tissue on PET," *American Journal of Roentgenology,* vol. 190, no. 5, pp. 1406-1409, 2008.

[8] A. Dimitrakopoulou-Strauss, L. Pan, and C. Sachpekidis, "Kinetic modeling and parametric imaging with dynamic PET for oncological applications: General considerations, current clinical applications, and future perspectives," *European Journal of Nuclear Medicine Molecular Imaging*, pp. 1-19, 2020.

[9] N. M. Freedman, S. K. Sundaram, K. Kurdziel, J. A. Carrasquillo, M. Whatley, J. M. Carson, D. Sellers, S. K. Libutti, J. C. Yang, and S. L. Bacharach, "Comparison of SUV and Patlak slope

for monitoring of cancer therapy using serial PET scans," *European journal of nuclear medicine molecular imaging,* vol. 30, no. 1, pp. 46-53, 2003.

[10] N. A. Karakatsanis, M. A. Lodge, A. K. Tahari, Y. Zhou, R. L. Wahl, and A. Rahmim, "Dynamic whole-body PET parametric imaging: I. Concept, acquisition protocol optimization and clinical application," *Physics in Medicine Biology,* vol. 58, no. 20, pp. 7391, 2013.

[11] N. A. Karakatsanis, Y. Zhou, M. A. Lodge, M. E. Casey, R. L. Wahl, H. Zaidi, and A. Rahmim, "Generalized whole-body Patlak parametric imaging for enhanced quantification in clinical PET," *Physics in Medicine Biology,* vol. 60, no. 22, pp. 8643, 2015.

[12] E. P. Visser, M. E. Philippens, L. Kienhorst, J. H. Kaanders, F. H. Corstens, L.-F. de Geus-Oei, and W. J. Oyen, "Comparison of tumor volumes derived from glucose metabolic rate maps and SUV maps in dynamic 18F-FDG PET," *Journal of Nuclear Medicine,* vol. 49, no. 6, pp. 892-898, 2008.

[13] G. Wang, A. Rahmim, and R. N. Gunn, "PET Parametric Imaging: Past, Present, and Future," *IEEE Transactions on Radiation Plasma Medical Sciences,* vol. 4, no. 6, pp. 663-675, 2020.

[14] C. S. Patlak, R. G. Blasberg, and J. D. Fenstermacher, "Graphical evaluation of blood-to-brain transfer constants from multiple-time uptake data," *Journal of Cerebral Blood Flow Metabolism,* vol. 3, no. 1, pp. 1-7, 1983.

[15] N. Desai, A. Singh, and D. J. Valentino, "Practical evaluation of image quality in computed radiographic (CR) imaging systems." p. 76224Q.